JACS
JOURNAL OF THE AMERICAN CHEMICAL SOCIETY
pubs.acs.org/JACS
Article

Thiophenol-Catalyzed Radical Hydroformylation of Unactivated Sterically Hindered Alkenes

Yisicheng Wang,[▽] Panpan Bao,[▽] Xiaojuan Dong,[▽] Yu Lan,* and Yiyun Chen*

Cite This: J. Am. Chem. Soc. 2025, 147, 31662−31670
Read Online
ACCESS | Metrics & More | Article Recommendations | Supporting Information

ABSTRACT: Sterically congested alkenes—ubiquitous in pharmaceuticals and industrial intermediates—remain inaccessible to classical hydroformylation due to prohibitive steric strain in transition-metal catalysis. Here, we report a thiophenol-catalyzed radical hydroformylation that overcomes dual steric and electronic constraints through a synergistic system: bench-stable α-chloro *N*-methoxyphthalimides (formyl precursors) and a tailored thiophenol HAT catalyst. This metal-free strategy achieves unprecedented hydroformylation of unactivated, tri-, and tetrasubstituted alkenes—including electron-rich styrenes and aliphatic alkene systems—with high chemo- and regioselectivity. Key advances include: 1) the first hydroformylation of tetrasubstituted styrenes, delivering β-aryl aldehydes with quaternary centers (up to 74% yield); 2) thiophenol lowers the HAT barrier by 8.3 kcal/mol to enable catalytic turnover under steric congestion. Mechanistic studies confirm a formyl radical pathway, while syngas (CO/H_2) elimination establishes a safe, sustainable platform for synthesizing medicinally relevant motifs (e.g., oxime ethers) and industrial targets like Lilial derivatives.

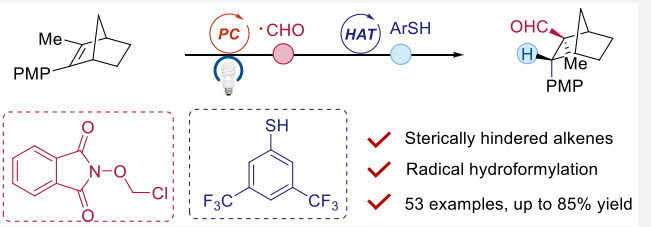

INTRODUCTION

Sterically congested aldehydes, including tertiary and quaternary alkyl-substituted variants, are prevalent in pharmaceuticals such as the antineoplastic agent peruvoside and the antifeedant dictyterpenoid A (Scheme 1a).[1] The aldehyde functional group embodies a dual role in medicinal chemistry: its intrinsic reactivity enables therapeutic activity but simultaneously risks metabolic instability and off-target covalent binding, leading to toxicity.[2] Safely leveraging aldehydes in drug design thus requires attenuating reactivity without compromising target engagement. A transformative strategy involves installing steric bulk at the α-position via methyl substitution, which spatially suppresses off-target interactions while preserving therapeutic function.[3] This principle is exemplified by genotoxicity studies of 3-(4-(*tert*-butyl)phenyl)propanal derivatives.[4] The α-unsubstituted congener was positive in the nucleophilic phospholipid (NPL) assay, indicating direct DNA damage. Remarkably, α-methylation abolished this genotoxic signal, with monomethyl substitution retaining only minimal residual bioactivity. While the bis-substituted congener remains untested due to unavailability, its increased steric shielding is hypothesized to further attenuate toxicity—a trend supported by the monosubstituted analogue's reduced activity. Despite the pharmacological relevance of sterically shielded aldehydes (e.g., bis-substituted derivatives), no general method exists for directly synthesizing these congested motifs from readily available alkenes—limiting their exploration and application in drug discovery.

Traditional hydroformylation methods, despite their industrial success, fail to address these medicinal chemistry demands. Hydroformylation, a cornerstone of industrial chemistry, converts alkenes into aldehydes at scale[5]—intermediates critical for polymers, pharmaceuticals, and agrochemicals.[6] However, these methods face three critical limitations: 1) the toxicity and handling risks of CO, restricting fine chemical synthesis;[7] 2) poor regiochemical control (linear vs branched products), particularly for styrenes where η^2-allyl metal intermediates favor branched isomers;[8] and 3) inefficacy with sterically congested alkenes.[9] While hydroformylation of mono- or disubstituted alkenes is well-precedented,[10] tri- and tetrasubstituted variants—especially those generating sterically hindered intermediates upon metal coordination—are unreactive, often yielding negligible results (Scheme 1b).[11] The direct synthesis of sterically hindered aldehydes from olefin precursors represents an economically compelling strategy to balance synthetic accessibility with controlled reactivity.

Radical hydroacylation offers a metal-free alternative to classical methods via a distinct reaction manifold, yet its utility has been constrained by two intertwined limitations: polarity mismatches and steric inaccessibility.[12] Nucleophilic acyl radicals exhibit preferential reactivity with electron-deficient alkenes (e.g., Michael acceptors, Scheme 1b),[13] while electron-

Received: May 2, 2025
Revised: August 5, 2025
Accepted: August 6, 2025
Published: August 21, 2025



Downloaded via SHANGHAI INST OF ORGANIC CHEMISTRY on October 15, 2025 at 01:13:28 (UTC).
See https://pubs.acs.org/sharingguidelines for options on how to legitimately share published articles.

© 2025 American Chemical Society

https://doi.org/10.1021/jacs.5c07415
J. Am. Chem. Soc. 2025, 147, 31662−31670

Scheme 1. Hydroformylation of Alkenes

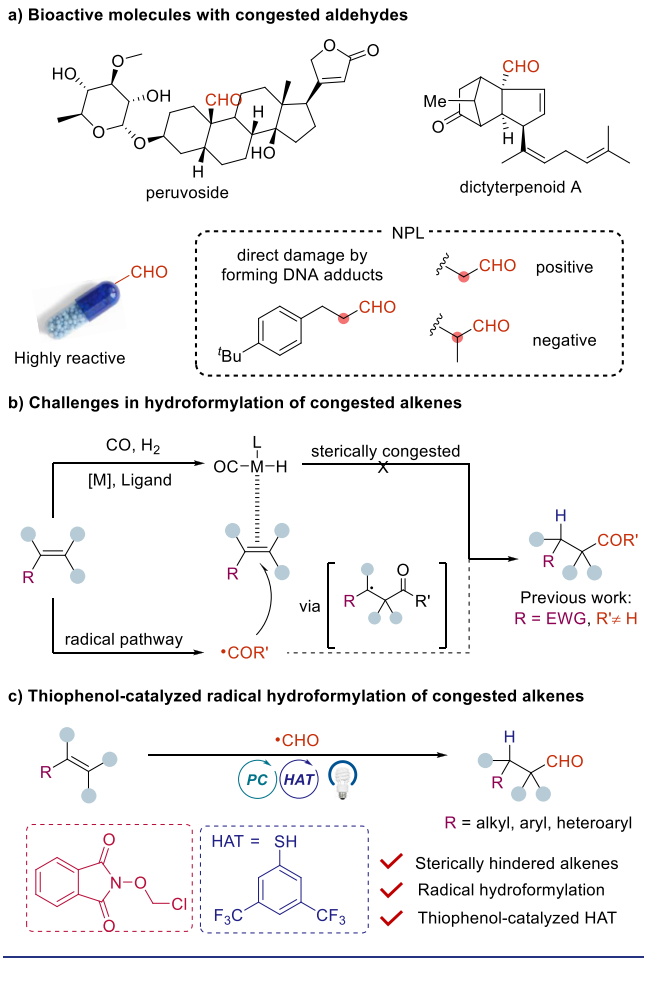

rich systems show limited reactivity due to incompatible frontier orbital interactions.[14] Furthermore, no existing radical hydroacylation method addresses unactivated sterically congested alkenes—a critical gap given their prevalence in pharmaceuticals and industrial feedstocks. This challenge extends to other acylative transformations (e.g., hydrocarboxylation),[15] where current strategies are restricted to tetrasubstituted Michael acceptors activated by strong electron-withdrawing groups (e.g., esters, ketones), leaving unactivated, sterically hindered alkenes unexplored.[16] Even our prior development of α-chloro *N*-methoxyphthalimides as bench-stable formyl radical precursors remained confined to electron-deficient alkenes,[17] as unresolved polarity mismatches precluded coupling with electron-rich or sterically shielded substrates. Collectively, these limitations underscore the unmet need for a general platform to functionalize inert, congested alkenes—a challenge central to this work.

To bridge this gap, we report a thiophenol-catalyzed hydrogen atom transfer (HAT) strategy that enables hydroformylation of mono- to tetrasubstituted alkenes—spanning electron-rich sterically hindered styrenes and unactivated aliphatic alkenes (Scheme 1c). This method directly resolves the dual limitations of polarity mismatches and steric congestion that have precluded radical hydrofunctionalization of electron-neutral and electron-rich alkenes. Mechanistically, the synergistic combination of α-chloro *N*-methoxyphthalimides (bench-stable formyl precursors) and a sterically attenuated thiophenol HAT catalyst lowers key energy barriers during catalytic turnover.[18] This synergy not only unlocks electronic constraints to functionalize electron-rich alkenes but also mitigates steric barriers that limit conventional HAT processes. This versatility positions the method as a general platform for synthesizing sterically demanding pharmaceuticals (e.g., quaternary carbon-containing aldehydes) and industrially relevant intermediates.

RESULTS AND DISCUSSION

Discovery of Thiophenol-Catalyzed Radical Hydroformylation of Alkene 1. We initiated our study with *p*-methoxystyrene (**1**) as the model substrate, combining it with α-chloro *N*-methoxyphthalimide (**2**),[19] Hantzsch ester (H2-HE) as a hydrogen donor, and *fac*-Ir(ppy)$_3$ as a photocatalyst under 468 nm blue LED irradiation in DCM (Table 1). While

Table 1. Reaction Optimization[a]

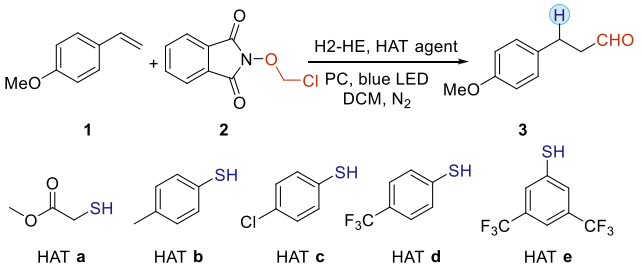

Entry	Conditions	Yield (%)[b]
1	*fac*-Ir(ppy)$_3$, no HAT agent	trace
2	HAT **a**	7
3	HAT **b**	18
4	HAT **c**	35
5	HAT **d**	39
6	HAT **e**	66(65)
7	entry 6, toluene	60(60)
8	entry 6, 4CzIPN	(72)
9	entry 8, freeze−thaw	(77)

[a]Reaction condition: **1** (0.1 mmol), **2** (0.2 mmol), *fac*-Ir(ppy)$_3$ (0.001 mmol), HAT reagent (0.02 mmol), and Hantzsch ester (0.3 mmol), in 2 mL DCM under nitrogen atmosphere with 2 × 4 W 468 nm blue LED irradiation at room temperature for 2 h. [b]Yields were determined by ^{1}H NMR analysis and isolated yields were in parentheses.

styrene **1** was fully consumed after 2 h, hydroformylation product formation was undetectable (<5% yield, entry 1). This stark discrepancy between substrate depletion and product yield indicated stalling at the radical intermediate stage, likely due to decomposition pathways. We reasoned that resonance delocalization from the phenyl ring stabilizes the benzylic radical intermediate, kinetically disfavoring the hydrogen atom transfer (HAT) step required for catalytic turnover. This stabilization mechanism—while beneficial in Michael acceptors by extending radical lifetimes[17]—paradoxically impedes efficient HAT in styrenic systems, halting chain propagation.

To overcome this HAT barrier, we systematically screened thiol-based catalysts, revealing substantial performance variations attributed to electronic and steric optimization (Scheme S1). Methyl thioglycolate (HAT **a**) afforded a marginal efficiency (7% yield, entry 2). Moderately improved yields were observed with *p*-toluenethiol (HAT **b**, 18%, entry 3). Substantial enhancement occurred using *p*-chlorothiophenol (HAT **c**, 35%, entry 4) and *p*-trifluoromethylthiophenol (HAT

https://doi.org/10.1021/jacs.5c07415
J. Am. Chem. Soc. 2025, 147, 31662−31670

Scheme 2. Scope of Mono- and Disubstituted Alkenes[a]

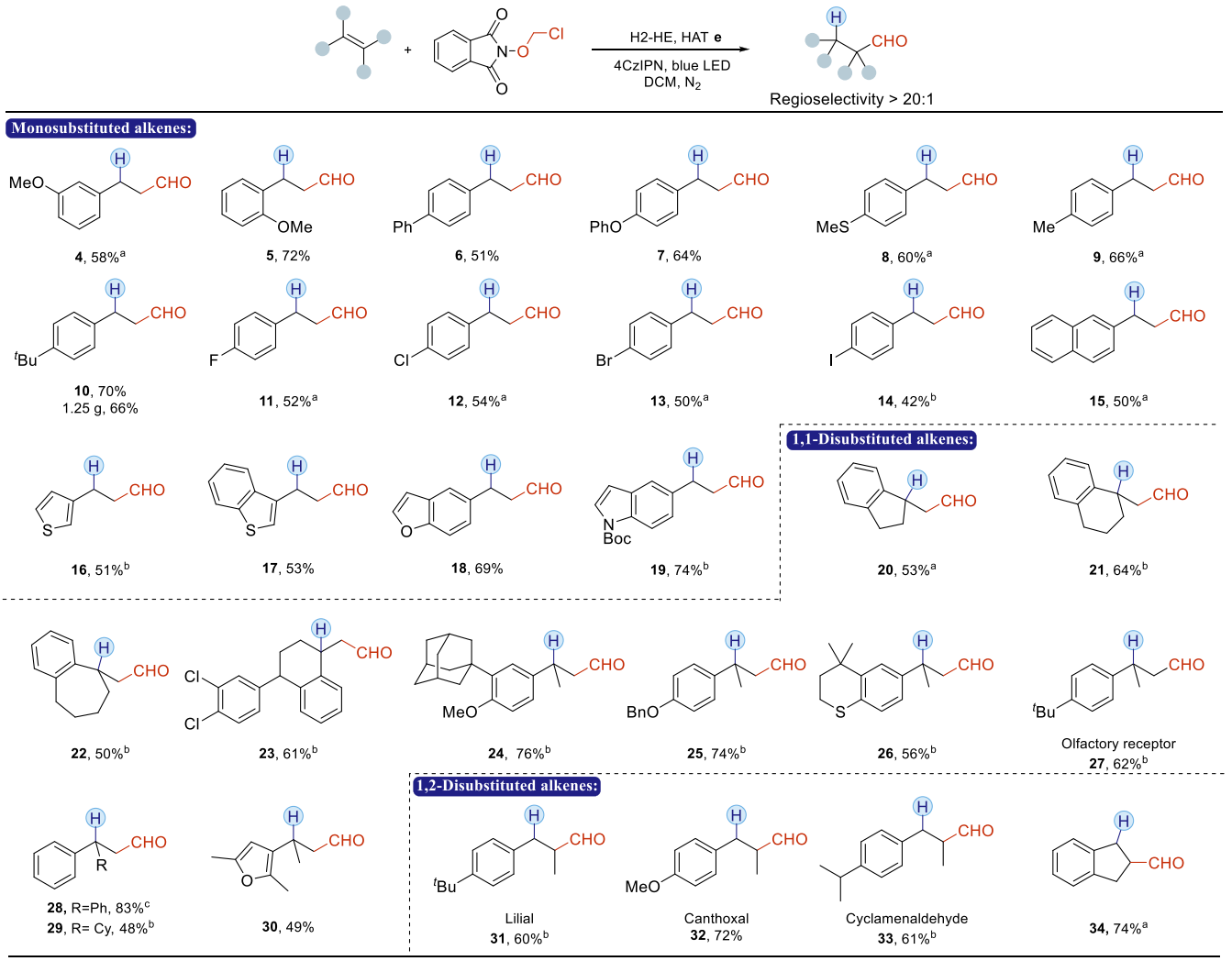

[a]**2** (0.6 mmol), Hantzsch ester (0.8 mmol). [b]**2** (0.6 mmol), Hantzsch ester (0.9 mmol). Reaction conditions: Alkene (0.2 mmol), **2** (0.4 mmol), 4CzIPN (0.002 mmol), HAT **e** (0.04 mmol), and Hantzsch ester (0.6 mmol) in 4 mL of DCM under a nitrogen atmosphere (freeze−thaw) with 2 × 4 W 468 nm blue LED irradiation at room temperature for 3 h. Isolated yields.

d, 39%, entry 5), where the electron-withdrawing groups increase thiyl radical electrophilicity. Crucially, 3,5-bis-(trifluoromethyl)benzenethiol (HAT **e**)[20] delivered 66% yield (65% isolated, entry 6)—a result attributed to optimal synergistic tuning: the two *meta*-CF_3 groups synergistically increase thiyl radical polarization while maintaining minimal steric hindrance with congested intermediates. Subsequent solvent optimization in toluene retained high efficiency (60% yield, entry 7), confirming the reaction's robustness to nonpolar media. Replacing *fac*-Ir(ppy)$_3$ with 4CzIPN further boosted the yield to 72% (entry 8), a result consistent with 4CzIPN's stronger reducing power.[21] Finally, rigorous deoxygenation of the reaction mixture elevated the isolated yield of aldehyde **3** to 77% (entry 9), underscoring the radical process's marginal sensitivity to oxygen quenching. This systematic optimization highlights how tailored catalyst design, solvent choice, and reaction engineering synergize to maximize the efficiency in radical hydroformylation.

Scope of Mono- and Disubstituted Alkenes. With the optimized conditions in hand, we evaluated the substrate scope of this radical hydroformylation method (Scheme 2). Monosubstituted styrenes with diverse arene substituents reacted efficiently: methoxy groups at meta- and ortho-positions provided aldehydes **4**−**5** in 58−72% yields, demonstrating tolerance for both electronic and steric variations. Electron-donating substituents—including phenyl (**6**, 51%), phenoxy (**7**, 64%), and methylthio (**8**, 60%)—performed well, despite their propensity to destabilize radical intermediates. Alkyl-substituted styrenes, such as methyl (**9**, 66%) and *tert*-butyl (**10**, 70%), were also viable, with the latter showcasing scalability in a gram-scale reaction that delivered 1.25 g of product **10** (66% yield). Halogenated styrenes exhibited robust compatibility across halogens—including fluorine, chlorine, and bromine (**11**−**13**, 50−54% yields)—and even iodide-substituted styrene (**14**, 42% yield).[22] Polycyclic aromatic and heteroaromatic alkenes underwent hydroformylation with remarkable efficiency: naphthalene (**15**, 50%), thiophene (**16**, 51%), benzothiophene (**17**, 53%), benzofuran (**18**, 69%), and indole (**19**, 74%) all furnished products in good yields.[23]

For 1,1-disubstituted alkenes,[24] our system exhibited exceptional regioselectivity across diverse scaffolds: exocyclic

https://doi.org/10.1021/jacs.5c07415
J. Am. Chem. Soc. 2025, 147, 31662−31670

Scheme 3. Scope of Congested and Unactivated alkenes[a]

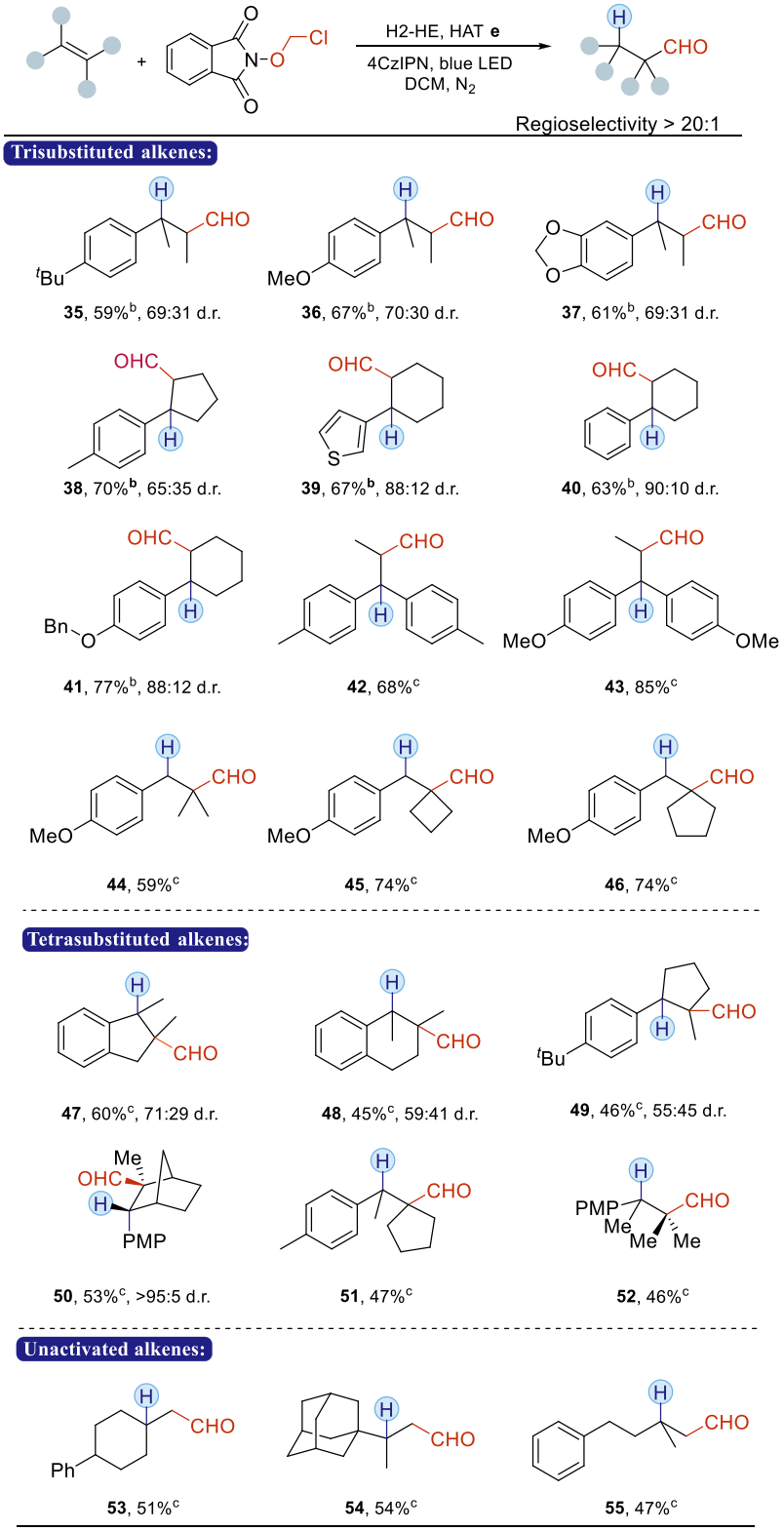

[a]**2** (0.6 mmol), Hantzsch ester (0.8 mmol). [b]**2** (0.6 mmol), Hantzsch ester (0.9 mmol). [c]See the Supporting Information for details. Reaction Condition: Alkene (0.2 mmol). **2** (0.4 mmol), 4CzIPN (0.002 mmol), HAT **e** (0.04 mmol), and Hantzsch ester (0.6 mmol), in 4 mL DCM under nitrogen atmosphere (freeze−thaw) with 2 × 4 W 468 nm blue LED irradiation at room temperature for 3 h. Isolated yields.

alkenes in five- (**20**), six- (**21**), and seven-membered rings (**22**) afforded aldehydes in 50−64% yields, while fused-ring systems (e.g., tetralin derivative **23**) achieved 61% yield. Noncyclic substrates **24**−**30** bearing bulky adamantyl or heteroaromatic substituents were also tolerated, delivering 49−83% yields. For 1,2-disubstituted alkenes, benzylic radical

https://doi.org/10.1021/jacs.5c07415
J. Am. Chem. Soc. 2025, 147, 31662−31670

stabilization enabled high regioselectivity toward 1-phenyl-substituted isopropanals (**31**−**33**, 60−72% yield)—valuable bioactive motifs widely used in fragrances and pharmaceuticals. A prime example is Lilial, a key aroma compound traditionally synthesized via a multistep sequence starting from *p-tert*-butylbenzaldehyde: condensation with propionaldehyde yields *p-tert*-butyl-2-methylcinnamaldehyde, which requires stringent hydrogenation conditions for final product isolation.[25] In contrast, our method enables a one-step synthesis of such aldehydes under mild conditions. Finally, indene was converted to aldehyde **34** in 74% yield, further demonstrating the method's versatility in handling sterically and electronically varied systems.

Scope of Congested and Unactivated Alkenes. Our method enables access to sterically congested aldehydes as bioactive building blocks (Scheme 3). For instance, trisubstituted alkenes were converted in 59−67% yields to obtain methyl-substituted derivatives of Lilial, Canthoxal, and cinnamic aldehydes **35**−**37**, with α-methylation likely enhancing their bioactivity.[3a] The protocol also accommodates cyclic scaffolds, such as cyclopentenyl (**38**, 70%) and cyclohexenyl derivatives (**39**−**41**, 63−77% yields)—key intermediates for synthesizing cyclopentanecarbaldehyde and cyclohexanecarbaldehyde, which are pivotal in pharmaceutical manufacturing. The method successfully accommodates sterically demanding 1,1-diaryl trisubstituted alkenes (**42**−**43**), delivering 68% and 85% yields, respectively, for sterically congested precursors of pheniramine-type antihistamine analogues. Our method's capacity to functionalize sterically demanding alkenes is exemplified by the synthesis of β-aryl *tert*-butyl aldehydes (**44**−**46**) in 59−74% yields.

Notably, this method achieves regioselective hydroformylation of cyclic tetrasubstituted alkenes, delivering sterically congested aldehydes **47**−**49** in 45−60% yields. The scope further encompasses highly strained systems: norbornene derivatives are efficiently converted to aldehyde **50** in 53% yield with exceptional diastereoselectivity (>95:5 d.r.), a transformation previously inaccessible. This advance holds broad relevance, as norbornene-based aldehydes are pivotal precursors in industrial chemistry, materials science, and asymmetric catalysis.[26] Exocyclic tetrasubstituted alkenes are similarly viable, affording aldehyde **51** in 47% yield. Crucially, regioselective hydroformylation of a congested acyclic tetrasubstituted alkene delivered aldehyde **52** in 46% yield—marking the efficient synthesis of a sterically congested Lilial derivative **32**.[27] Prior acylative transformations remain exclusively limited to tetrasubstituted Michael acceptors activated by electron-withdrawing groups (e.g., esters, ketones),[16] while hydroacylation and hydrocarboxylation of unactivated tetrasubstituted alkenes constitute largely an unexplored territory.[15] It is against this constrained landscape that our methodology's unique capability emerges—enabling acylative functionalization of sterically encumbered, unactivated alkenes without electronic activation.

Having established success with sterically hindered styrenic systems, we next targeted unactivated aliphatic alkenes—substrates exhibiting limited reactivity toward radical addition under standard conditions.[28] These challenging systems initially showed sluggish reactivity, affording only modest yields. However, increasing the equivalents of the formyl radical precursor (α-chloro *N*-methoxyphthalimide) significantly enhanced efficiency, delivering aldehydes **53**−**55** in 47−54% yields. This optimization highlights the method's adaptability: by tuning precursor loading to compensate for the inherently low reactivity of unactivated aliphatic alkenes, we expand hydroformylation's scope to those challenging systems.

Synthetic Transformations of α-Quaternary Aldehydes. The sterically shielded aldehydes synthesized via our method serve as versatile platforms for constructing bioactive hindered functionalities through streamlined transformations (Scheme 4). For instance, aldehyde **45**—bearing a quaternary carbon center—was converted in one step to oxime ether **56** (97% yield), a motif prevalent in antiviral and anticancer agents.[29] Furthermore, a classical Wittig reaction with **45** delivered sterically encumbered olefin **57** in 82% yield, demonstrating retained reactivity, even under high steric demand. Remarkably, a two-step protocol involving **45** enabled access to α-quaternary nitrile **58** (88% yield), a structural element with emerging applications in Parkinson's disease therapeutics.[30] Additionally, reductive amination of **45** furnished amine **59** (77% yield), a critical moiety in a renin inhibitor candidate designed to engage the enzyme's S3′ subsite.[31] These transformations underscore the method's dual advantage: preserving steric complexity, critical for metabolic stability, while enabling diversification into drug-like scaffolds with minimal synthetic effort.

Scheme 4. Synthetic Transformations of α-Quaternary Aldehydes

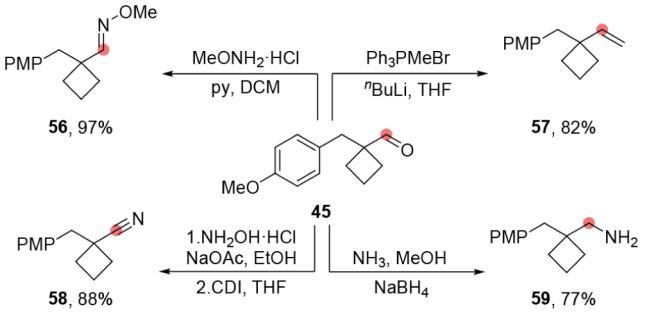

Mechanistic Investigations and Proposed Reaction Mechanism. To elucidate the reaction mechanism, we conducted a series of mechanistic investigations (Scheme 5). Radical clock studies employing a cyclopropane-substituted alkene **60** provided direct evidence for radical intermediates via the formation of ring-opened product **61** (Scheme 5a).[32] Critically, deuterium labeling studies distinguished the hydrogen source: when α-chloro *N*-methoxyphthalimide ([D2]-**62**) was used, exclusive (>99%) incorporation of deuterium into the aldehyde **63** formyl proton was observed (Scheme 5b). Conversely, deuterium labeling experiments using [D2]-Hantzsch ester ([D2]-HE) **64** revealed negligible deuterium incorporation (<5%) in the aldehyde product **3** (Scheme 5b). This mechanistic divergence starkly contrasts with prior observations in Michael acceptor systems lacking thiophenol additives, where significant deuteration at the aldehyde β-position was observed by using [D2]-HE **64** (Scheme S2). Collectively, these findings confirm that thiophenol supplants Hantzsch ester as the HAT agent in this system, enabling catalytic turnover of the alkyl radical intermediate generated after formyl addition. This represents a fundamental mechanistic divergence from the Michael acceptor paradigm,

https://doi.org/10.1021/jacs.5c07415
J. Am. Chem. Soc. 2025, 147, 31662−31670

Scheme 5. Mechanistic Investigations and Proposed Reaction Mechanism

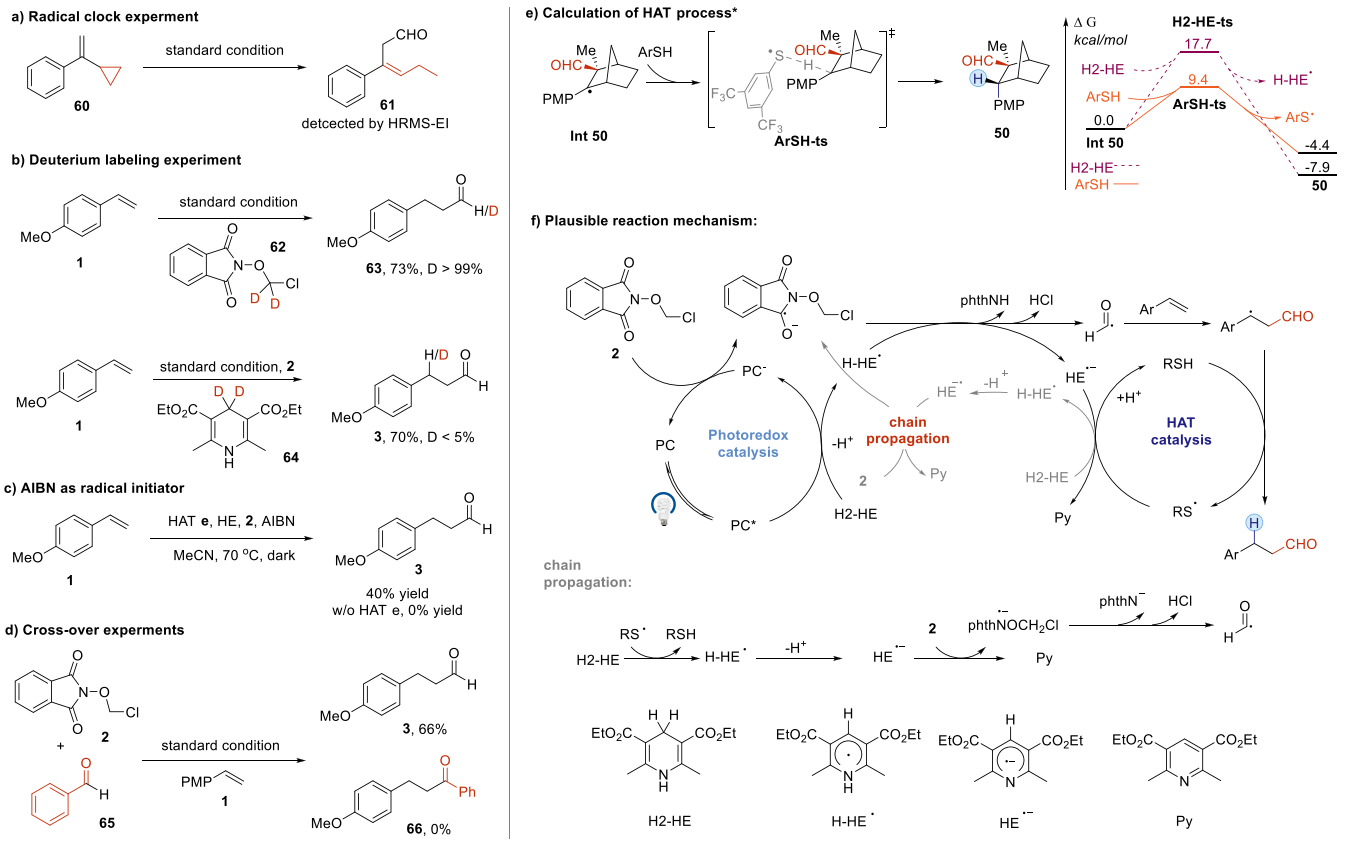

where Hantzsch ester participates directly in hydrogen atom transfer.[17]

Furthermore, a quantum yield of Φ = 6.1 (>1) strongly supports a radical chain propagation mechanism.[33] To further probe the chain process, we conducted reactions using thermal initiation with 2,2'-azobis(2-methylpropionitrile) (AIBN).[34] Crucially, in the presence of a thiophenol catalyst (HAT **e**), hydroformylation adduct **3** was obtained in 40% yield. In stark contrast, the omission of HAT **e** completely suppressed product formation (Scheme 5c), unequivocally demonstrating the thiophenol's indispensable role in sustaining the radical chain. This dependency diverges fundamentally from Michael acceptor systems under identical AIBN conditions, where thiophenol is dispensable for productive turnover (Table S4). Crossover experiments using benzaldehyde detected no benzoin addition products, ruling out formaldehyde as a viable hydroformylation intermediate (Scheme 5d). Radical trapping with TEMPO or BHT completely suppressed product formation, further corroborating a radical-based pathway (Section S3.10).[35]

The hydrogen atom transfer (HAT) step—critical for sustaining catalytic turnover—emerged as the key bottleneck in sterically congested systems. Computational analysis (M06-2X/6-31G(d)/IEF-PCM$_{(dichloromethane)}$) reveals that employing a sterically tailored thiophenol HAT catalyst reduces the energy barrier for **Int 50** to 9.4 kcal/mol, a 8.3 kcal/mol improvement over the prohibitively high barrier of the direct HAT pathway with Hantzsch ester (H2-HE, 17.7 kcal/mol, Scheme 5e). This dramatic reduction arises from the thiophenol's dual role: 1) its electron-deficient aryl ring polarizes the transition state, accelerating HAT, while 2) steric tailoring minimizes repulsive interactions between the catalyst and the bulky substrate. This mechanistic synergy between formyl radical precursors and tailored HAT agents is the linchpin for efficient catalytic turnover, enabling the hydroformylation of substrates previously deemed inaccessible to both radical and metal-catalyzed methods.

Based on cumulative experimental and computational evidence, we propose the reaction mechanism depicted in Scheme 5f. The reaction begins with a single-electron transfer from the photoexcited catalyst to α-chloro *N*-methoxyphthalimide, generating a radical anion that undergoes N−O bond cleavage to release phthalimide and an α-chloromethoxyl radical.[36] Subsequent concerted elimination of HCl from this α-chloromethoxyl radical releases the key formyl radical. This formyl species adds regioselectively across the alkene to generate an alkyl radical.[37] Crucially, this alkyl radical abstracts hydrogen from the thiophenol catalyst (HAT **e**), delivering the aldehyde product while forming a thiyl radical. The radical chain propagates when the thiyl radical abstracts a hydrogen atom from the Hantzsch ester (H2-HE; $\Delta G^{\ddagger}$ = 5.7 kcal/mol, Figure S10). This generates the Hantzsch ester radical (H-HE$^{\bullet}$, E(H-HE$^{\bullet}$/PyH^{+})= −0.72 V vs SCE in MeCN, Figure S5) while regenerating the thiophenol catalyst.[38] Subsequent deprotonation of H-HE$^{\bullet}$ forms the strongly reducing Hantzsch ester radical anion (HE$^{\bullet-}$, E(H-HE$^{\bullet-}$/Py) = −2.06 V vs SCE in MeCN, Figure S6),[39] which reduces phthalimide (E(**2**/**2**$^{\bullet-}$) = −1.28 V vs SCE in MeCN, Figure S7) to drive formyl radical generation. DFT calculations exclude chloromethoxyl radical addition due to unfavorable nucleophile−nucleophile pairing with alkenes ($\Delta\omega$ = 0.17 eV vs formyl radical, Figure S8).

https://doi.org/10.1021/jacs.5c07415
J. Am. Chem. Soc. 2025, 147, 31662−31670

CONCLUSIONS

In summary, we present a thiophenol-catalyzed, metal-free radical hydroformylation strategy that converts sterically congested alkenes—including tri-/tetrasubstituted styrenes lacking electron-withdrawing groups and unactivated aliphatic alkenes—into aldehydes using α-chloro *N*-methoxyphthalimides as formyl radical precursors. Key to this advance is the thiophenol HAT catalyst, which lowers the reaction barrier by 8.3 kcal/mol ($\Delta\Delta G^{\ddagger}$ = 9.4 vs 17.7 kcal/mol for direct HAT), enabling efficient catalytic turnover under steric congestion. By eliminating syngas (CO/H_2), this method provides safe, sustainable access to sterically shielded aldehydes, including β-aryl aldehydes with quaternary carbon centers and cyclic carbaldehydes—motifs critical to drug design (e.g., *tert*-butyl aldehydes) and industrial intermediates (e.g., Lilial analogues). By resolving long-standing steric and electronic limitations, this work bridges gaps in synthetic methodology while offering a sustainable alternative to classical hydroformylation with direct implications for drug discovery, green chemistry, and industrial process development.

ASSOCIATED CONTENT

Supporting Information

The Supporting Information is available free of charge at https://pubs.acs.org/doi/10.1021/jacs.5c07415.

Experimental procedures, reaction optimizations, detailed mechanistic investigations, and new compound characterizations (PDF)

AUTHOR INFORMATION

Corresponding Authors

Yiyun Chen − *State Key Laboratory of Chemical Biology, Shanghai Institute of Organic Chemistry, University of Chinese Academy of Sciences, Shanghai 200032, China; School of Physical Science and Technology, ShanghaiTech University, Shanghai 201210, China; School of Chemistry and Material Sciences, Hangzhou Institute for Advanced Study, University of Chinese Academy of Sciences, Hangzhou 310024, China*; orcid.org/0000-0003-0916-0994; Email: yiyunchen@sioc.ac.cn

Yu Lan − *College of Chemistry, and Pingyuan Laboratory, Zhengzhou University, Zhengzhou, Henan 450001, China; School of Chemistry and Chemical Engineering, Chongqing Key Laboratory of Chemical Theory and Mechanism, Chongqing University, Chongqing 401331, China*; orcid.org/0000-0002-2328-0020; Email: lanyu@cqu.edu.cn

Authors

Yisicheng Wang − *State Key Laboratory of Chemical Biology, Shanghai Institute of Organic Chemistry, University of Chinese Academy of Sciences, Shanghai 200032, China; School of Physical Science and Technology, ShanghaiTech University, Shanghai 201210, China*

Panpan Bao − *College of Chemistry, and Pingyuan Laboratory, Zhengzhou University, Zhengzhou, Henan 450001, China*

Xiaojuan Dong − *State Key Laboratory of Chemical Biology, Shanghai Institute of Organic Chemistry, University of Chinese Academy of Sciences, Shanghai 200032, China; Central China Normal University, Wuhan, Hubei 430079, China*

Complete contact information is available at: https://pubs.acs.org/10.1021/jacs.5c07415

Author Contributions

[▽]Y.W., P.B., and X.D. contributed equally to this work.

Notes

The authors declare no competing financial interest.

ACKNOWLEDGMENTS

Financial support was provided by the National Natural Science Foundation of China (22337005, 22277133), the Strategic Priority Research Program of the Chinese Academy of Sciences (XDB1060000), and the Youth Innovation Promotion Association CAS (2023266).

REFERENCES

(1) (a) Reddy, D.; Kumavath, R.; Tan, T. Z.; Ampasala, D. R.; Kumar, A. P. Peruvoside targets apoptosis and autophagy through MAPK Wnt/β-catenin and PI3K/AKT/mTOR signaling pathways in human cancers. *Life Sci.* **2020**, *241*, 117147. (b) Suzuki, M.; Yamada, H.; Kurata, K. Dictyterpenoids A and B, Two Novel Diterpenoids with Feeding-Deterrent Activity from the Brown Alga Dilophus okamurae. *J. Nat. Prod.* **2002**, *65*, 121−125.

(2) O'Brien, P. J.; Siraki, A. G.; Shangari, N. Aldehyde Sources, Metabolism, Molecular Toxicity Mechanisms, and Possible Effects on Human Health. *Crit. Rev. Toxicol.* **2005**, *35*, 609−662.

(3) (a) Sun, S.; Fu, J. Methyl-containing pharmaceuticals: Methylation in drug design. *Bioorg. Med. Chem. Lett.* **2018**, *28*, 3283−3289. (b) Gampe, C.; Verma, V. A. Curse or Cure? A Perspective on the Developability of Aldehydes as Active Pharmaceutical Ingredients. *J. Med. Chem.* **2020**, *63*, 14357−14381. (c) Casi, G.; Huguenin-Dezot, N.; Zuberbühler, K.; Scheuermann, J.; Neri, D. Site-Specific Traceless Coupling of Potent Cytotoxic Drugs to Recombinant Antibodies for Pharmacodelivery. *J. Am. Chem. Soc.* **2012**, *134*, 5887−5892.

(4) Kobets, T.; Duan, J.-D.; Brunnemann, K. D.; Iatropoulos, M. J.; Etter, S.; Hickey, C.; Smith, B.; Williams, G. M. In ovo testing of flavor and fragrance materials in Turkey Egg Genotoxicity Assay (TEGA), comparison of results to in vitro and in vivo data. *Food Chem. Toxicol.* **2018**, *115*, 228−243.

(5) (a) Franke, R.; Selent, D.; Börner, A. Applied Hydroformylation. *Chem. Rev.* **2012**, *112*, 5675−5732. (b) Zhang, B.; Peña Fuentes, D.; Börner, A. Hydroformylation. *ChemTexts* **2022**, *8*, 2.

(6) (a) Chen, M.; Gupta, G.; Ordonez, C. W.; Lamkins, A. R.; Ward, C. J.; Abolafia, C. A.; Zhang, B.; Roling, L. T.; Huang, W. Intermetallic Nanocatalyst for Highly Active Heterogeneous Hydroformylation. *J. Am. Chem. Soc.* **2021**, *143*, 20907−20915. (b) Nurttila, S. S.; Linnebank, P. R.; Krachko, T.; Reek, J. N. H. Supramolecular Approaches To Control Activity and Selectivity in Hydroformylation Catalysis. *ACS Catal.* **2018**, *8*, 3469−3488.

(7) (a) Delolo, F. G.; Almeida, L. D.; Vieira, G. M.; dos Santos, E. N.; Gusevskaya, E. V. Green Solvents in Hydroformylation-based Processes and Other Carbonylation Reactions. *Green Chem.* **2025**, *27*, 4816−4866. (b) Pandey, S.; Raj, K. V.; Shinde, D. R.; Vanka, K.; Kashyap, V.; Kurungot, S.; Vinod, C. P.; Chikkali, S. H. Iron Catalyzed Hydroformylation of Alkenes under Mild Conditions: Evidence of an Fe(II) Catalyzed Process. *J. Am. Chem. Soc.* **2018**, *140*, 4430−4439.

(8) (a) Zhang, X.; Yan, T.; Hou, H.; Yin, J.; Wan, H.; Sun, X.; Zhang, Q.; Sun, F.; Wei, Y.; Dong, M.; Fan, W.; Wang, J.; Sun, Y.; Zhou, X.; Wu, K.; Yang, Y.; Li, Y.; Cao, Z. Regioselective hydroformylation of propene catalysed by rhodium-zeolite. *Nature* **2024**, *629*, 597−602. (b) Huang, H.; Yu, C.; Zhang, Y.; Zhang, Y.; Mariano, P. S.; Wang, W. Chemo- and Regioselective Organo-Photoredox Catalyzed Hydroformylation of Styrenes via a Radical Pathway. *J. Am. Chem. Soc.* **2017**, *139*, 9799−9802.

(9) (a) Zhang, D.; Zheng, J.; You, C.; Li, L.; Chung, L. W.; Zhou, Q.; Li, S.; Ren, T.; Yang, Y.; Zhang, X.; Li, X. Catalytic Regio- and Enantioselective Hydroformylation of Trisubstituted Alkenes to Construct α-Quaternary Lactams. *J. Am. Chem. Soc.* **2025**, *147*, 7886−7896. (b) Zhu, Y.; Zhang, Y.; He, D.; Yang, H.; Xue, X.-S.; Tang, W. Rhodium-Catalyzed Asymmetric Reductive Hydroformylation of α-Substituted Enamides. *J. Am. Chem. Soc.* **2024**, *146*, 33249−33257. (c) Li, S.; Zhang, D.; Purushothaman, A.; Lv, H.; Shilpa, S.; Sunoj, R. B.; Li, X.; Zhang, X. Chemo-, regio- and enantioselective hydroformylation of trisubstituted cyclopropenes: access to chiral quaternary cyclopropanes. *Nat. Commun.* **2024**, *15*, 6377.

(10) (a) Yan, Y.; Zhang, X. A Hybrid Phosphorus Ligand for Highly Enantioselective Asymmetric Hydroformylation. *J. Am. Chem. Soc.* **2006**, *128*, 7198−7202. (b) Noonan, G. M.; Fuentes, J. A.; Cobley, C. J.; Clarke, M. L. An Asymmetric Hydroformylation Catalyst that Delivers Branched Aldehydes from Alkyl Alkenes. *Angew. Chem., Int. Ed.* **2012**, *51*, 2477−2480.

(11) (a) Dydio, P.; Reek, J. N. H. Supramolecular Control of Selectivity in Hydroformylation of Vinyl Arenes: Easy Access to Valuable β-Aldehyde Intermediates. *Angew. Chem., Int. Ed.* **2013**, *52*, 3878−3882. (b) Li, S.; Zhang, D.; Zhang, R.; Bai, S. -T.; Zhang, X. Rhodium-Catalyzed Chemo-, Regio- and Enantioselective Hydroformylation of Cyclopropyl-Functionalized Trisubstituted Alkenes. *Angew. Chem., Int. Ed.* **2022**, *61*, No. e202206577. (c) Shin, T.; Kim, H.; Kim, S.; Lee, A.; Seo, M.-S.; Choi, J.; Kim, H.; Kim, H. Ligand-Controlled Direct Hydroformylation of Trisubstituted Olefins. *Org. Lett.* **2019**, *21*, 5789−5792.

(12) (a) Chatgilialoglu, C.; Crich, D.; Komatsu, M.; Ryu, I. Chemistry of Acyl Radicals. *Chem. Rev.* **1999**, *99*, 1991−2070. (b) Chudasama, V.; Fitzmaurice, R. J.; Caddick, S. Hydroacylation of α,β-unsaturated esters via aerobic C−H activation. *Nat. Chem.* **2010**, *2*, 592−596. (c) Zhang, X.; MacMillan, D. W. C. Direct Aldehyde C−H Arylation and Alkylation via the Combination of Nickel, Hydrogen Atom Transfer, and Photoredox Catalysis. *J. Am. Chem. Soc.* **2017**, *139*, 11353−11356. (d) Budai, B.; Leclair, A.; Wang, Q.; Zhu, J. Copper-Catalyzed 1,2-Methoxy Methoxycarbonylation of Alkenes with Methyl Formate. *Angew. Chem., Int. Ed.* **2019**, *131*, 10411−10415.

(13) (a) Yan, J.; Tang, H.; Kuek, E. J. R.; Shi, X.; Liu, C.; Zhang, M.; Piper, J. L.; Duan, S.; Wu, J. Divergent functionalization of aldehydes photocatalyzed by neutral eosin Y with sulfone reagents. *Nat. Commun.* **2021**, *12*, 7214. (b) Garwood, J. J. A.; Chen, A. D.; Nagib, D. A. Radical Polarity. *J. Am. Chem. Soc.* **2024**, *146*, 28034−28059.

(14) (a) Giese, B. Formation of CC Bonds by Addition of Free Radicals to Alkenes. *Angew. Chem., Int. Ed.* **1983**, *22*, 753−764. (b) Paul, S.; Filippini, D.; Silvi, M. Polarity Transduction Enables the Formal Electronically Mismatched Radical Addition to Alkenes. *J. Am. Chem. Soc.* **2023**, *145*, 2773−2778.

(15) (a) Willis, M. C. Transition Metal Catalyzed Alkene and Alkyne Hydroacylation. *Chem. Rev.* **2010**, *110*, 725−748. (b) Li, J. H.; Shi, Y. A. Progress on transition metal catalyzed asymmetric hydroesterification, hydrocarboxylation, and hydroamidation reactions of olefins. *Chem. Soc. Rev.* **2022**, *51*, 6757−6773.

(16) (a) Alkayal, A.; Tabas, V.; Montanaro, S.; Wright, I. A.; Malkov, A. V.; Buckley, B. R. Harnessing Applied Potential: Selective β-Hydrocarboxylation of Substituted Olefins. *J. Am. Chem. Soc.* **2020**, *142*, 1780−1785. (b) Moteki, S. A.; Usui, A.; Selvakumar, S.; Zhang, T. X.; Maruoka, K. Metal-Free C-H Bond Activation of Branched Aldehydes with a Hypervalent Iodine(III) Catalyst under Visible-Light Photolysis: Successful Trapping with Electron-Deficient Olefins. *Angew. Chem., Int. Ed.* **2014**, *53*, 11060−11064. (c) Malandain, A.; Molins, M.; Hauwelle, A.; Talbot, A.; Loreau, O.; D'Anfray, T.; Goutal, S.; Tournier, N.; Taran, F.; Caillé, F.; Audisio, D. Carbon Dioxide Radical Anion by Photoinduced Equilibration between Formate Salts and [^{11}C, ^{13}C, ^{14}C]CO_2: Application to Carbon Isotope Radiolabeling. *J. Am. Chem. Soc.* **2023**, *145*, 16760−16770.

(17) Liu, D.; Yang, K.; Fang, D.; Li, S. J.; Lan, Y.; Chen, Y. Formyl Radical Generation from α-Chloro N-Methoxyphthalimides Enables Selective Aldehyde Synthesis. *Angew. Chem., Int. Ed.* **2023**, *62*, No. e202213686.

(18) Romero, N. A.; Nicewicz, D. A. Mechanistic Insight into the Photoredox Catalysis of Anti-Markovnikov Alkene Hydrofunctionalization Reactions. *J. Am. Chem. Soc.* **2014**, *136*, 17024−17035.

(19) Liu, D.; Chen, Y. 2-(Chloromethoxy)-1H-isoindole-1,3(2H)-dione. In *Encyclopedia of Reagents for Organic Synthesis*; John Wiley & Sons, Inc, 2024.

(20) (a) Zhou, W.; Dmitriev, I. A.; Melchiorre, P. Reductive Cross-Coupling of Olefins via a Radical Pathway. *J. Am. Chem. Soc.* **2023**, *145*, 25098−25102. (b) Cuthbertson, J. D.; MacMillan, D. W. C. The direct arylation of allylic sp3 C−H bonds via organic and photoredox catalysis. *Nature* **2015**, *519*, 74−77. (c) Capacci, A. G.; Malinowski, J. T.; McAlpine, N. J.; Kuhne, J.; MacMillan, D. W. C. Direct, enantioselective α-alkylation of aldehydes using simple olefins. *Nat. Chem.* **2017**, *9*, 1073−1077.

(21) Speckmeier, E.; Fischer, T. G.; Zeitler, K. A Toolbox Approach To Construct Broadly Applicable Metal-Free Catalysts for Photoredox Chemistry: Deliberate Tuning of Redox Potentials and Importance of Halogens in Donor−Acceptor Cyanoarenes. *J. Am. Chem. Soc.* **2018**, *140*, 15353−15365.

(22) Ren, W.; Chang, W.; Dai, J.; Shi, Y.; Li, J.; Shi, Y. An Effective Pd-Catalyzed Regioselective Hydroformylation of Olefins with Formic Acid. *J. Am. Chem. Soc.* **2016**, *138*, 14864−14867.

(23) Tanaka, R.; Nakano, K.; Nozaki, K. Synthesis of α-Heteroarylpropanoic Acid via Asymmetric Hydroformylation Catalyzed by Rh(I)-(R,S)-BINAPHOS and the Subsequent Oxidation. *J. Org. Chem.* **2007**, *72*, 8671−8676.

(24) Deng, Y.; Wang, H.; Sun, Y.; Wang, X. Principles and Applications of Enantioselective Hydroformylation of Terminal Disubstituted Alkenes. *ACS Catal.* **2015**, *5*, 6828−6837.

(25) Carpenter, M. S.; Easter, W. M., Jr; Hasbrouck Heights, N. J. *4-tert-butyl alpha-methyl hydrocinnamic aldehyde*; US 2,875,131 A, 1959.

(26) (a) Zhang, C.; Zhang, X.; Zou, J.-J.; Li, G. Catalytic dimerization of norbornadiene and norbornene into hydrocarbons with multiple bridge rings for potential high-density fuels. *Coord. Chem. Rev.* **2021**, *436*, 213779. (b) Wang, J.; Dong, G. Palladium/Norbornene Cooperative Catalysis. *Chem. Rev.* **2019**, *119*, 7478−7528.

(27) (a) Sunada, Y.; Ogushi, H.; Yamamoto, T.; Uto, S.; Sawano, M.; Tahara, A.; Tanaka, H.; Shiota, Y.; Yoshizawa, K.; Nagashima, H. Disilaruthena- and Ferracyclic Complexes Containing Isocyanide Ligands as Effective Catalysts for Hydrogenation of Unfunctionalized Sterically Hindered Alkenes. *J. Am. Chem. Soc.* **2018**, *140*, 4119−4134. (b) Lu, H. X.; Wang, C.; Gao, T. T.; Lin, E. Z.; Lu, S. L.; Hong, X.; Li, B. J. Rhodium-Catalyzed Highly Enantioselective Hydroboration of Acyclic Tetrasubstituted Alkenes Directed by an Amide. *J. Am. Chem. Soc.* **2024**, *146*, 16194−16202.

(28) (a) Song, L.; Wang, W.; Yue, J.-P.; Jiang, Y.-X.; Wei, M.-K.; Zhang, H.-P.; Yan, S.-S.; Liao, L.-L.; Yu, D.-G. Visible-light photocatalytic di- and hydro-carboxylation of unactivated alkenes with CO2. *Nat. Catal.* **2022**, *5*, 832−838. (b) Bai, Z.; Zhang, H.; Wang, H.; Yu, H.; Chen, G.; He, G. Enantioselective Alkylamination of Unactivated Alkenes under Copper Catalysis. *J. Am. Chem. Soc.* **2021**, *143*, 1195−1202. (c) Wang, Z.-C.; Luo, X.; Zhang, J.-W.; Liu, C.-F.; Koh, M. J.; Shi, S.-L. Enantioselective C−C cross-coupling of unactivated alkenes. *Nat. Catal.* **2023**, *6* (6), 1087−1097.

(29) Kosmalski, T.; Kupczyk, D.; Baumgart, S.; Paprocka, R.; Studzińska, R. A Review of Biologically Active Oxime Ethers. *Molecules* **2023**, *28*, 5041.

(30) Candito, D. A.; Simov, V.; Gulati, A.; Kattar, S.; Chau, R. W.; Lapointe, B. T.; Methot, J. L.; DeMong, D. E.; Graham, T. H.; Kurukulasuriya, R.; Keylor, M. H.; Tong, L.; Morriello, G. J.; Acton, J. J.; Pio, B.; Liu, W.; Scott, J. D.; Ardolino, M. J.; Martinot, T. A.; Maddess, M. L.; Yan, X.; Gunaydin, H.; Palte, R. L.; McMinn, S. E.; Nogle, L.; Yu, H.; Minnihan, E. C.; Lesburg, C. A.; Liu, P.; Su, J.; Hegde, L. G.; Moy, L. Y.; Woodhouse, J. D.; Faltus, R.; Xiong, T.; Ciaccio, P.; Piesvaux, J. A.; Otte, K. M.; Kennedy, M. E.; Bennett, D. J.; DiMauro, E. F.; Fell, M. J.; Neelamkavil, S.; Wood, H. B.; Fuller, P.

https://doi.org/10.1021/jacs.5c07415
J. Am. Chem. Soc. 2025, 147, 31662−31670

H.; Ellis, J. M. Discovery and Optimization of Potent, Selective, and Brain-Penetrant 1-Heteroaryl-1H-Indazole LRRK2 Kinase Inhibitors for the Treatment of Parkinson's Disease. *J. Med. Chem.* **2022**, *65*, 16801−16817.
(31) Sun, X.; Wen, X.; Chen, Y.-Y.; Shi, C.; Gao, C.; Wu, Y.; Wang, L.-J.; Yang, X.-H.; Sun, H. Discovery of highly potent renin inhibitors potentially interacting with the S3′ subsite of renin. *Eur. J. Med. Chem.* **2015**, *103*, 269−288.
(32) Beckwith, A. L. J.; Bowry, V. W. Kinetics of Reactions of Cyclopropylcarbinyl Radicals and Alkoxycarbonyl Radicals Containing Stabilizing Substituents: Implications for Their Use as Radical Clocks. *J. Am. Chem. Soc.* **1994**, *116*, 2710−2716.
(33) Cismesia, M. A.; Yoon, T. P. Characterizing chain processes in visible light photoredox catalysis. *Chem. Sci.* **2015**, *6*, 5426−5434.
(34) Escoubet, S.; Gastaldi, S.; Vanthuyne, N.; Gil, G.; Siri, D.; Bertrand, M. P. Thiyl Radical Mediated Racemization of Non-activated Aliphatic Amines. *J. Org. Chem.* **2006**, *71*, 7288−7292.
(35) (a) Beejapur, H. A.; Zhang, Q.; Hu, K.; Zhu, L.; Wang, J.; Ye, Z. TEMPO in Chemical Transformations: From Homogeneous to Heterogeneous. *ACS Catal.* **2019**, *9*, 2777−2830. (b) Yehye, W. A.; Rahman, N. A.; Ariffin, A.; Abd Hamid, S. B.; Alhadi, A. A.; Kadir, F. A.; Yaeghoobi, M. Understanding the chemistry behind the antioxidant activities of butylated hydroxytoluene (BHT): A review. *Eur. J. Med. Chem.* **2015**, *101*, 295−312.
(36) (a) Kaiser, E. W.; Wallington, T. J. FTIR Product Study of the Cl-Initiated Oxidation of CH3Cl: Evidence for HCl Elimination from the Chloromethoxy Radical. *J. Phys. Chem.* **1994**, *98*, 5679−5685. (b) Niki, H.; Maker, P. D.; Savage, C. M.; Breitenbach, L. P. An FTIR study of the Cl atom-initiated oxidation of CH2Cl2 and CH3Cl. *Int. J. Chem. Kinet.* **1980**, *12*, 1001−1012. (c) Zhang, J.; Li, Y.; Xu, R.; Chen, Y. Donor−Acceptor Complex Enables Alkoxyl Radical Generation for Metal-Free C(sp3)−C(sp3) Cleavage and Allylation/Alkenylation. *Angew. Chem., Int. Ed.* **2017**, *56*, 12619−12623.
(37) (a) Wang, P.-Z.; Chen, J.-R.; Xiao, W.-J. Hantzsch esters: an emerging versatile class of reagents in photoredox catalyzed organic synthesis. *Org. Biomol. Chem.* **2019**, *17*, 6936−6951. (b) Qiu, G.; Knowles, R. R. Understanding Chemoselectivity in Proton-Coupled Electron Transfer: A Kinetic Study of Amide and Thiol Activation. *J. Am. Chem. Soc.* **2019**, *141*, 16574−16578.
(38) Su, Y.-L.; Liu, G.-X.; Liu, J.-W.; Tram, L.; Qiu, H.; Doyle, M. P. Radical-Mediated Strategies for the Functionalization of Alkenes with Diazo Compounds. *J. Am. Chem. Soc.* **2020**, *142*, 13846−13855.
(39) (a) Shen, G.-B.; Fu, Y.-H.; Zhu, X.-Q. Thermodynamic Network Cards of Hantzsch Ester, Benzothiazoline, and Dihydrophenanthridine Releasing Two Hydrogen Atoms or Ions on 20 Elementary Steps. *J. Org. Chem.* **2020**, *85*, 12535−12543. (b) Yuan, L.; Shen, G. -B.; Fu, Y. -H.; Zhu, X. -Q. What are the differences between Hantzsch ester and H_2 as two-hydrogen-atom donors in acetonitrile on the thermodynamics of elementary steps? *J. Phys. Org. Chem.* **2017**, *30*, No. e3599.

NOTE ADDED AFTER ASAP PUBLICATION

This article published ASAP on August 21, 2025. Due to production error, Schemes 1, 2, 3, 5, Table 1 and Table of Contents/Abstract graphics have been replaced. The corrected version reposted on August 22, 2025.



https://doi.org/10.1021/jacs.5c07415
J. Am. Chem. Soc. 2025, 147, 31662−31670